Ge Gao

Shelter Effect Study Of Wind-driven Rain On Building Facade

Beiträge aus der Architektur

Ge Gao

Shelter Effect Study Of Wind-driven Rain On Building Facade

VOGT

Dresden 2015

Bibliografische Information der Deutschen Nationalbibliothek
Die Deutsche Nationalbibliothek verzeichnet diese Publikation in der Deutschen Nationalbibliografie; detaillierte bibliografische Daten sind im Internet über http://dnb.dnb.de abrufbar.

Bibliographic Information published by the Deutsche Nationalbibliothek
The Deutsche Nationalbibliothek lists this publication in the Deutsche Nationalbibliografie; detailed bibliographic data are available on the Internet at http://dnb.dnb.de.

Zugl.: Dresden, Techn. Univ., Diss., 2015

Die vorliegende Arbeit stimmt mit dem Original der Dissertation „Shelter Effect Study Of Wind-driven Rain On Building Facade“ von Ge Gao überein.

Gesetzt vom Autor

ISBN 978-3-938860-86-1

Jörg Vogt Verlag
Niederwaldstr. 36
01277 Dresden
Germany

Phone: +49-(0)351-31403921
Telefax: +49-(0)351-31403918
e-mail: info@vogtverlag.de
Internet : www.vogtverlag.de

Shelter Effect Study Of Wind-driven Rain On Building Facade

For achievement of the academic degree

Doctor of Engineering(Dr.-Ing.)

Faculty of Architecture

Dresden University of Technology

PHD thesis submitted by

M.sc. Ge Gao

born on March 13th 1979 in Jilin, China

Supervisors: Prof. Dr.-Ing. John Grunewald

Prof. Dr. Lihua Zhao

Date of defence: October 29th 2014

“Nothing in the world can take the place of persistence. Talent will not; nothing is more common than unsuccessful men with talent. Genius will not; unrewarded genius is almost a proverb. Education will not; the world is full of educated derelicts. Persistence and determination alone are omnipotent. The slogan, ‘press on’ has solved, and always will solve, the problems of the human race.” -Calvin Coolidge

Preface and Acknowledgement

The work outlined in this thesis has been accomplished during my research studies at the institute of Building Climatology, Dresden University of Technology in the years of 2008 to 2014. The my study is firstly inspired by Prof. Xu's question: Although there are a lot of studies up to now in the field of hygrothermal transport modelling in the porous medium, is the boundary conditions inputted in to the simulation software accurate enough? After reviewing a number of literatures about boundary conditions, I narrowed down my study topic and focused my research on the wind-driven rain, the water boundary condition.

Prof. John Grunalwald and my colleague Heike Fechner introduced me to the latest developments: wind-driven rain model used in Delphin. As there are still some limitations on this model, the aim of this study is to develop a time-variable wind-driven rain model which takes more considerations into account and can be easily implemented in hygrothermal transport calculation software. It is very lucky for me that I found a study topic whose results can be used by Delphin. And this interesting topic also made it possible for me to complete Ph.D. research in IBK (Institute of Building Climatology).

During the process of writing my thesis, there are some persons I would like to thank. First and foremost I want to thank my advisor Prof. John Grunewald. I appreciate all his contributions of time, ideas, and funding to make my Ph.D. experience productive and stimulating. Thank him for his sincere interest in my topic of research and for giving me the opportunity to become part of the building climatology group. The joy and enthusiasm he has for his research was contagious and motivational for me, even during tough times in the Ph.D. pursuit. He has given guidance and invested many hours in closely reviewing abstracts, papers and this dissertation. He also gave me abundant freedom to follow my own research interests, which has always supported and promoted.

I will forever be thankful to my former supervisor, Prof. Yugong Xu, who brought me into a new research field, I feel very fortunate that I could base my thesis on his intriguing idea.

Much gratitude also goes towards my other supervisors, Prof. Lihua Zhao and who was always open for discussions and patiently answered all my questions. I am also thankful for the excellent example she has provided as a successful woman scientists.

I gratefully acknowledge the funding sources that made my Ph.D. work possible. I was funded by China Scholarship Council CSC for my first year in Germany.

My gratitude goes to Dr. Rudolf Plagge for his support, guidance, and discussions during research process.

I would also like to express my thanks to Prof. Peter Haeupl for his support and encouragement.

I would also like to thank the other two members of my oral defense committee, Prof. Joerg Rainer Noennig, Prof. Bernhard Weller.

I further would like to thank Heiko Fechner for the effort he putted in my presentation preparation and provided constructive advices.

I would like to thank all my colleagues who not only were always open for stimulating discussions, but foremost for creating a friendly and supportive environment. This includes Peggy Freudenberg, Anita Morandell Meissner, Margitta Thurow-Langer, Jianhua Zhao, Magdi Khalil, Zile Jia. Andrea Vasquez, Magdalena Tarkiewicz. Lots of thanks are due to Ting Zhang, who sacrificed her weekends for expertly proof-reading this thesis and for her comments and questions about my work.

I would also thank my friend Tang Tang for his help for data processing and model implementation.

Finally, I thank my family for all their love and encouragement. For my parents who raised me with a love of science and supported me in all my pursuits. I will also thank my mother, father and sister in law, for their support and encouragement. And most of all for my supportive, encouraging and patient husband Changshan Wang whose faithful support throughout this research. I also thank Changshan for sharing literature and for our theoretical discussions. Thanks to my son Elias for supporting me on his own way and giving me perspective in life.

Abstract

Wind-driven rain is defined as the quantity of rain that passes through a plane with defined orientation in the atmosphere. It is well known that rain water (wind-driven rain) causes more than 90% critical damage to buildings. As the most important boundary condition, wind-driven rain has significant effect on the accuracy of hygrothermal building component simulation. The existing wind-driven rain estimation approaches have limits. They are either: 1) over simplified and cannot capture comprehensive essential effects, or 2) too complicate to perform. The aim of the present study is to develop a new wind-driven rain model, WDR-Pdr model. Field measurement, CFD (Computational Fluid Dynamics) simulation and statistical analysis are used in this study. By using WDR-Pdr model wind driven rain on building façades in street canyon can be estimated. During the study of the wind-driven rain model, more influencing factors such as the density of buildings and the arrangements of the surrounding buildings are taken into account. Based on observations and statistical analysis, the correlation between wind pressure and wind –driven rain was studied out. As a result, a new parameter, wind pressure Pdr, is used in this new model which is in conjunction with M.Grosso's wind pressure model. As a parametric model, WDR-Pdr model is convenient to use and it economize the complicated processes of CFD simulation and data processing.

Contents

1 Overview of Wind-driven Rain Research **1**

1.1 Overview of Wind-driven Rain 1

1.1.1 Description of WDR on building façade 1

1.1.2 Why WDR matters 2

1.2 Research status of WDR 4

1.2.1 Experimental study 4

1.2.2 Semi-empirical study 7

1.2.3 Numerical study of WDR 13

1.2.4 Statistical study of WDR 14

1.2.5 Discussions and conclusions 15

1.3 The significance of wind-driven rain research in urban areas 17

1.3.1 Urbanization und microclimate in urban areas 17

1.3.2 WDR research on the process of China's urbanization 18

1.4 Introduction to the new WDR model research 22

1.4.1 Objective of this work 22

1.4.2 Research methodologies 23

1.5 Outline of the thesis 23

2 Atmospheric Boundary Layer Simulation **25**

2.1 Introduction 25

2.2 ABL flow simulation 27

2.2.1 Introduction of the ABL flow 27

2.2.2 Core issues and the strategy of ABL simulation 28

2.2.3 Basic requirements of accurate ABL simulation 29

2.2.4 Modelling of ABL 29

2.3 The ABL effect on WDR 36

2.3.1 Numerical model 37

2.3.2 Results of ABL simulation 38

2.3.3 WDR simulation model and the influence of ABL flow on WDR simulation . . . 39
2.4 Conclusions . . . 45

3 Wind-driven Rain in the Urban Environment 47
3.1 Introduction . . . 47
3.2 CFD validation of wind field in urban environment . . . 49
3.2.1 Wind tunnel experiment . . . 49
3.2.2 Boundary conditions . . . 50
3.2.3 Turbulence models and model setting . . . 50
3.2.4 Validation of CFD simulation . . . 51
3.3 Measurement of WDR in dense city area . . . 52
3.3.1 Test object chosen . . . 53
3.3.2 Wind and horizontal rain intensity measurement . . . 54
3.3.3 Fabrication and installation of test equipment of Wind-driven rain 54
3.3.4 Measurement results analysis . . . 55
3.3.5 WDR simulation of test case . . . 58
3.4 Comparison with the simulation results by Blocken . . . 66
3.5 Discussions . . . 69
3.6 Conclusions . . . 70

4 Shelter Effect on Wind Field and Driving Rain Intensity 71
4.1 Introduction . . . 71
4.2 Introduction of the simulation cases . . . 72
4.3 Shelter effect on the wind field . . . 74
4.3.1 Wind field in different shelter styles . . . 74
4.3.2 Wind field in different packing densities . . . 76
4.4 Shelter effect on the Wind-driven rain . . . 77
4.4.1 Raindrops trajectories analysis . . . 77
4.4.2 Catch ratios on buildings' facades . . . 79
4.5 Conclusions . . . 80

5 Statistics Analysis on the WDR Influencing Factors 83
5.1 Introduction . . . 83
5.2 The description of the influencing factors . . . 84
5.3 Sensitivity analysis . . . 85
5.3.1 Horizontal rain intensity sensitivity . . . 85

5.3.2 Packing density sensitivity . . . 85
5.3.3 Shelter style sensitivity . . . 86
5.3.4 Wind direction sensitivity . . . 86
5.3.5 Wind velocity sensitivity . . . 87
5.3.6 Conclusions . . . 87
5.4 Correlation analysis . . . 88
5.4.1 Introduction of correlation theory . . . 88
5.4.2 Correlations . . . 89
5.5 Regression analysis on the WDR influencing factors . . . 92
5.5.1 The comparison of the regression lines . . . 92
5.5.2 Discussions on the results of WDR regression analysis . . . 93
5.6 Conclusions . . . 95

6 The Development and Implementation of a New WDR Model: WDR-Pdr model 97
6.1 Introduction . . . 97
6.2 $WDR - P_{dr}$model . . . 97
6.2.1 The introduction of WDR calculation coefficients database . . . 98
6.2.2 The selection of the parametric wind pressure model . . . 99
6.3 Parameters and their calculation methods in WDR-Pdr model . . . 104
6.3.1 Dimensions of building and its environment . . . 104
6.3.2 Meteorological data . . . 104
6.3.3 Topography factor . . . 105
6.4 The outline of WDR-Pdr model application . . . 106
6.5 Application example of WDR model . . . 107
6.6 The implementation of the new WDR model and conclusions . . . 110
6.6.1 Program flow chart . . . 111
6.6.2 Implementation results . . . 112
6.7 conclusions . . . 113

7 Conclusions and Perspectives 115

A Vantage Pro2 Wireless 117

B Rain Water Amount on Test Building Facades 121
B.1 Rain water amount collected by gauges . . . 121
B.2 Rain water amount from simulation . . . 123

C Wind Field Charts **127**
C.1 Wind field profiles in different arrangements . . . 128
C.2 Wind field profiles in different densities . . . 130
C.3 Comparison of shelter style . . . 131
C.3.1 Comparison of Ux approaching building facade . . . 131
C.3.2 Comparison of Uz on building surface . . . 132
C.3.3 Comparison of Uy on building surface . . . 133
C.4 Comparison of building densities (CBST) . . . 134

D Charts of the Rain Intensity Distribution on Cubic Building Facades **137**
D.1 On building facade in different arrangements . . . 138
D.2 On building facade in different horizontal rain intensities . . . 140

E Charts of the Sensitivity and Correlation Analysis **143**
E.1 Horizontal rain intensity sensitivity analysis . . . 143
E.2 Packing density sensitivity analysis . . . 146
E.3 Shelter style sensitivity . . . 149
E.4 Wind velocity influencing analysis . . . 151
E.5 Catch ratio scatter points . . . 156

F Catch Ratio and Pdr Regression Plots **159**
F.1 D=0 degrees . . . 159
F.2 D=22.5 degrees . . . 162
F.3 D=45 degrees . . . 165
F.4 D=67.5 degrees . . . 168

G Coefficients for the Wind Pressure Calculation Equations **172**
G.1 $C_{f\alpha}$ . . . 172
G.2 $C_{f\lambda p\bar{y}}(\lambda_p)$ . . . 172
G.3 $C_{fD}(\bar{x}, \bar{y})$ . . . 173
G.4 C_{fRaf} . . . 174
G.5 C_{fRas} . . . 175

H Implementation Code **178**
H.1 Realization with matlab code . . . 178

List of Tables

1.1 HAM tools . . . 3
1.2 WDR coefficient α . . . 10
1.3 Obstruction factors(ISO (2009)) . . . 10
1.4 WDR coefficient α . . . 12
1.5 Wind velocity exposure and height factors (EHF) (Straube (2010)) . . . 12
1.6 Comparison of the catch ratio values . . . 16

2.1 Turbulent model constants for various flows . . . 30
2.2 Exponents for different upwind exposure . . . 31
2.3 Classification of terrains by their roughness length, partially adapted from the European Wind Atlas . . . 31
2.4 Parameters of the wind flow . . . 37
2.5 Boundary conditions of the basic numerical model . . . 38

3.1 Statistic of building height distribution over Hong Kong (Yim (2009)) . . . 49
3.2 Model setting for the validation of flow field in city areas (MODWF=modified wall function, BIA=Building influence area) . . . 51
3.3 Shelter effect test result . . . 56
3.4 Grid refinement . . . 62
3.5 Comparison of WDR models between Blocken and author . . . 67
3.6 Relative catch ratio values at position 1 in Figure 3.4.1 . . . 68

4.1 Description of simulation cases . . . 73

5.1 Introduction of simulation cases . . . 84
5.2 Independent variables . . . 89
5.3 Correlations between CR and variables . . . 90
5.4 Correlations between $P_{dr}$and CR . . . 90
5.5 Independent variables . . . 91
5.6 Correlations among CR and influencing factors . . . 92

5.7 Regression table for different included angels 94

6.1 Influencing parameters in M.Grosso model 101
6.2 Formulas for correction factors in M.Grosso model 102
6.3 Parameters for speed-up over hills and escarpments 105
6.4 $C_{Pdrnorm}(\bar{y})$ reults for example case 108
6.5 $C_{f\lambda p\bar{y}}$ reults for example case 108
6.6 $C_{fD\bar{y}}$ results for example case 109
6.7 CF results for example case 109
6.8 $P_{\bar{x}\bar{y}}$ results for example case 109
6.9 $CR_{\bar{x}\bar{y}}$ results for example case 110
6.10 R_{WDR} results for example case 110

A.1 Integrated sensor suite (ISS) 120
A.2 Data displayed on console 120

G.1 Coefficients for $C_{f\alpha}(\bar{x}, \bar{y})$ 172
G.2 Coefficients for $C_{f\lambda p\bar{y}}(\lambda_p)$ 172
G.3 Coefficients for $C_{fD\bar{y}}(\overline{x})$ 173
G.4 Coefficients for $C_{fRaf}(Raf, \bar{y})$ 174
G.5 Coefficients for C_{fRaf} 175
G.6 Coefficients for $C_{fRas}(Ras, \lambda_p, \bar{y})(Ras < 1)$ 176
G.7 Coefficients for $C_{fRas}(Ras, \lambda_p, \bar{y})(Ras > 1)$ 177

List of Symbols

Roman symbols

A	$[-]$	constant by experiment in the definition of β
A_f	$[m^2]$	the total frontal area of cubes
A_p	$[m^2]$	the total plan area of the cubes
A_t	$[m^2]$	the total floor area
C_p	$[-]$	surface pressure coefficient
C_r	$[-]$	constant in W calculation equation
C_D	$[-]$	the drag coefficient for a spherical droplet
$C_{f\lambda p\bar{y}}$	$[-]$	packing density correction factor
$C_{fD\bar{y}}$	$[-]$	direction correction factor
$C_{Pdrnorm}$	$[-]$	the wind dynamic pressure on the isolated building facade
C_t	$[-]$	the topograph wind velocity correction factor
CF	$[-]$	global C_p correction factor
CR	$[-]$	rainfall catch ratio
$CR_{i,coarse}$	$[-]$	catch ratio calculated value with coarse mesh
$CR_{i,middle}$	$[-]$	catch ratio calculated value with middle mesh
$CR_{i,fine}$	$[-]$	catch ratio calculated value with fine mesh
D	$[m]$	raindrop's diameter
D	$[\circ]$	the main wind direction
$F(D)$	$[-]$	the fraction of liquid water in the air
F_D	$[S^{-1}]$	the inverse of the relaxation time
F1....F5	$[-]$	the vertical positions on building facade
H	$[m]$	the height of the building

K_m	$[m2/s]$	eddy viscosity coefficient
L	$[m]$	the length of the building
L_h	$[m]$	topographic geometric values
O	$[-]$	the obstruction factor
P	$[pa]$	the air pressure
P_{dr}	$[pa]$	the wind dynamic pressure
p_{ref}	$[pa]$	the reference wind dynamic pressure
R	$[-]$	the convergence ratio
R_{dr}	$[mm/h]$	rain intensity on the building facade
Re	$[-]$	the relative Reynolds number
R_h	$[mm/h]$	the horizontal rain intensity
R_v	$[mm/h]$	the free driving rain intensity
RH_{avg}	$[mm/h]$	the average rain intensity during one rain fall event on horizontal surface
RU_{avg}	$[mm/h]$	the average rain intensity on the unsheltered building facade
RS_{avg}	$[mm/h]$	the average rain intensity on the sheltered building facade
$S1....S12$	$[-]$	the horizontal positions on building facade
S_{max}	$[-]$	the factor used in C_t calculation equation
S_x	$[m]$	the space between buildings in x direction
S_y	$[m]$	the space between buildings in y direction
U_{ref}	$[m/s]$	the reference wind speed
Ux	$[m/s]$	the approaching wind velocity in x direction
Uy	$[m/s]$	the approaching wind velocity in y direction
Uz	$[m/s]$	the approaching wind velocity in z direction
$\overline{V}$	$[m/s]$	mean parts of the horizontal velocity

V'	$[m/s]$	the turbulent part of the horizontal velocity
$V_{rainterminal}$	$[m/s]$	the terminal velocity of rain drop
$V_{rainmax}$	$[m/s]$	the constant in $V_{rainterminal}$ calculation equation
ABL	$[-]$	the atmosphere boundary layer
WDR	$[-]$	the wind driven rain
W	$\left[mm^3/m^3\right]$	the amount of liquid water in the unit volume of space
W	$[m]$	the width of building
a	$[-]$	coefficients for theC_t calculation equation
a_1, a_2, a_3	$[-]$	coefficients for the C_D calculation equation
b	$[-]$	constant by experiment in the definition of β
e	$[-]$	coefficients for the$V_{rainterminal}$ calculation equation
f	$\left[s^{-1}\right]$	Coriolis parameter
f_i	$[-]$	the computed solution on mesh i
h_i	$[m]$	the characteristic grid spacing
g	$[-]$	the constant in calculation equation
k	$\left[m^2/s^2\right]$	turbulent energy
k	$[-]$	the factor used in C_t calculation equation
p	$[-]$	the order of accuracy
q	$[-]$	constant in $V_{rainterminal}$ calculation equation
r	$[-]$	constant in W calculation equation
$\overline{u}$	$[-]$	horizontal flow in x direction
u^*_{ABL}	$[m/s]$	the ABL friction velocity
$\overrightarrow{u_p}$	$[m/s]$	the particle velocity vector
u_*	$[m/s]$	friction velocity

u'	$[m/s]$	the turbulent component in x direction
$\overline{v}$	$[m/s]$	horizontal flow in y direction
v_{avg}	$[m/s]$	the average wind velocity
v_{coarse}	$[m/s]$	wind velocity with coarse mesh
v_{middle}	$[m/s]$	wind velocity with middle mesh
v_{fine}	$[m/s]$	wind velocity with fine mesh
x	$[m]$	the distance from the crest
$\overline{x}$	$[-]$	non-dimensional position in x direction
$\overline{y}$	$[-]$	non-dimensional position in y direction
z	$[m]$	the height above the ground
z	$[m]$	the height above the crest
z_0	$[m]$	the aerodynamic roughness length
k	$[-]$	Karman's constant
r	$[-]$	constant in W calculation equation

Greek symbols

α	$[s/m]$	coefficient for the calculation of the free driving rain intensity
α_d	$[\circ]$	the displacement shielding angle
α_h	$[\circ]$	horizontal shielding angle
α_v	$[\circ]$	vertical shielding angle
β	$[-]$	constant in rain drops's diameter distribution equation
γ	$[-]$	constant by experiment in the definition of β
μ	$\left[NS/m^2\right]$	the molecular viscosity of the air
ε	$\left[m^2/s^3\right]$	the turbulent dissipation rate
ω'	$[m/s]$	the turbulent component in y direction
η	$[-]$	the fraction of the rain intensity
ξ'	$[m]$	characteristic distance
δ_i	$[-]$	the spatial discretization error of the quantity on mesh i
φ_h	$\left[h^{-1}\right]$	horizontal drop mass spectrum
ρ	$\left[kg/m^3\right]$	the density of air
ρ_{air}	$\left[kg/m^3\right]$	the density of air
ρ_p	$\left[kg/m^3\right]$	the density of particle
λ_f	$[-]$	the frontal packing density
λ_p	$[-]$	the packing density

1 Overview of Wind-driven Rain Research

1.1 Overview of Wind-driven Rain

1.1.1 Description of WDR on building façade

The term 'wind-driven rain' (WDR), also known as 'driven rain', originally comes from the research of earth science and meteorology. It refers to the rain that is given a horizontal velocity by the wind and that falls obliquely Blocken (2004). Figure 1.1.1 is the sketch about reproduction of the co-occurrence of wind and rain.

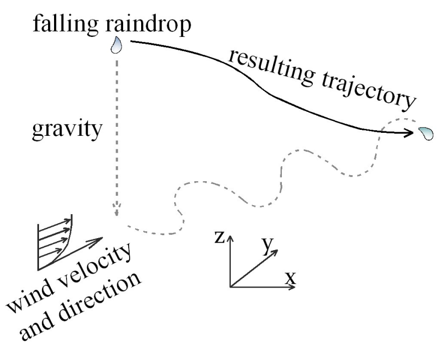

Figure 1.1.1: Diagram of WDR

According to positions and orientations of the collection devices (shown as Figure 1.1.2), WDR values can be classified into three different parameters: the horizontal rain intensity R_h, verticle rain intensity R_v and wind-driven rain intensity on the building facade R_{dr}.

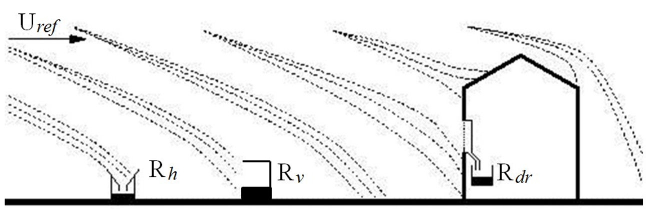

Figure 1.1.2: Diagram of WDR collection gauges

1.1.2 Why WDR matters

Impact of WDR on the building facade

The amount of rain water which impinged on the building envelope has a significant effect on the durability of buildings' structures (Jacobsen & Matala (1996), Sereda & Litvan (1980)), the appearance of building's surface (Dario & Ottavio (1982), Camuffo (1992), Davidson & Etyemezian (2000), De Freitas & Delgado (2013)), the building envelope's thermal performance , the indoor air humidity (Sanders & Kumaraperumal (2008), Abuku & Roels (2007), De Freitas & Delgado (2013)) and the users' health and comfort. The previous study by Karagiozis & Kuenzel (2003) indicates that among all weather-related damages, more than 90% critical damages to buildings are caused by WDR. As the effects of the damages caused by WDR might be hidden within the structure of the buildings and might be delayed, the caused losses are hard to estimate. Apart from the negative aspects mentioned above, there are also some positive effects the buildings can benefit from. In some hot and rainy zones, e.g. South China and South East Asia, the WDR on the building facade can also have a cooling effect. With the evaporation of the rain water on the building's envelope, the heat can be taken away. Appropriately designed and structured overhangs or other assemblies which can collect WDR are applied in some green buildings. In United States, the rainwater harvesting system is factored into the evaluation of green building. In this sense, the WDR research has practical significance in both reducing its negative effects on humans and the using of resources.

WDR application in Energy and HAM tools

Acquiring the WDR value can help wall designers: 1) estimate the response of the wall assembly to the WDR; 2) determine the design WDR loads of the wall assembly; 3) assess the degree of damage caused by WDR on the assembly (Teasdale-St-Hilaire & Derome (2006), Lacasse (2003)).

In addition to the applications mentioned above, the WDR loads estimation methodology could also be used in building energy simulation (BES) and heat and moisture transport (HAM) tools. Over the last five decades, hundreds of building energy estimation tools have been developed and used. A list of such tools can be obtained on the US Department of Energy Webpage (USDEW (2013)). This directory provides information of more than 400 building softwares with variable subjects: energy simulation, envelope systems, HVAC equipment and systems, energy economics, etc. As a very important aspect of the overall performance of buildings, heat, air and moisture (HAM) transfer processes in the building envelope are supposed to be calculated accurately in the whole building simulation models. However the predictions of moisture transfer process are not well considered in most current building energy simulation tools. According to the list of building energy software tools (USDEW (2013)), as Figure 1.1.3 shows, among the 411 building calculation tools, there are only 11 tools which take moisture transfer process into account.

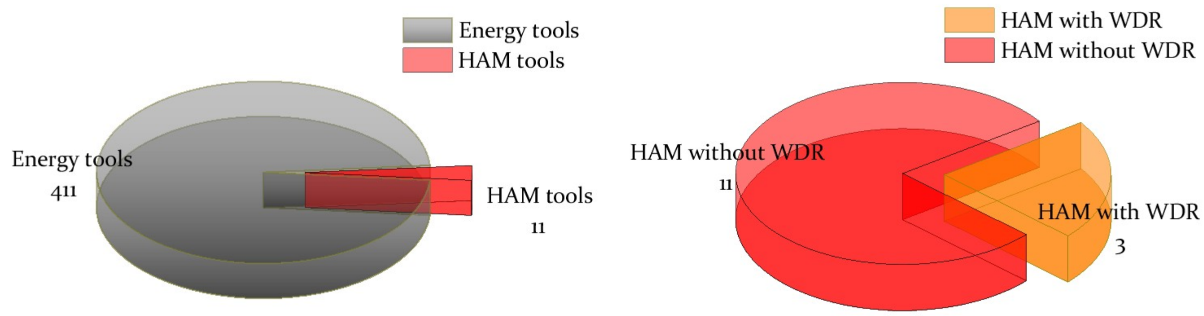

Figure 1.1.3: Energy and HAM tools

Table 1.1: HAM tools

Name	Boundary conditions (exterior)		
	Wind	Rain intensity (vertical)	WDR
1D-HAM	No	No	No
Bsim2000	Yes	No	No
DELPHIN	Yes	Yes	Yes
EMPTIED	No	No	No
GLASTA	No	No	No
hygiRC-1D	Yes	Yes	No
HAMLab	Yes	Yes	Yes
HAM-tools	Yes	Yes	No(possible with simplified models)
IDA-ICE	Yes	No	No
MATCH	Yes	Yes	No
MOIST	Yes	No	No
MOIST-EXP	Yes	Yes	No
UMIDUS	Yes	No	No
WUFI	Yes	Yes	Yes

The HAM processes include exchange between exterior and interior climate, and heat and moisture transport within building components. The boundary conditions imposed on a mathematical model are often as critical to its accuracy as the proper modeling of the moisture environment. WDR is the most important moisture sources for building façade, and its intensity acts as an essential boundary condition for the HAM transfer models (Blocken & Carmeliet (2004), Sanders (1996)). However WDR is not widely applied in HAM or BES calculation. In the frame work of Annex41, among 17 HAM models only 5 tools take the rain intensity as a boundary condition. (Woloszyn & Rode (2008)). As shown in Table 1.1 and Figure 1.1.3, even in the public HAM softwares, the WDR intensity is rarely taken into account (De Freitas & Delgado (2013)).

However, according to research of Abuku (Abuku & Janssen (2008)) in 2008, WDR has significant impacts on energy consumption, indoor relative humidity and mold growth. Ignoring the effect of WDR may cause great error when conducting HAM calculation.

1.2 Research status of WDR

Bert Blocken (Blocken & Carmeliet (2005)) classified the WDR study into two parts: WDR loads studies and the response of the target building to WDR. In this thesis the studies are focused on WDR loads and the results implementation in HAM tools. Typically, there are three kinds of methods of WDR loads research including experimental study, semi-empirical studies, numerical and statistical study.

1.2.1 Experimental study

A comprehensive and systematic review about the WDR experimented study has been conducted by Bert Blocken (Blocken & Carmeliet (2004)). In this subsection, the development of WDR study is briefly introduced. Originally, earth scientists and meteorologist (Philos (1816), Knox (1837), and Symons & F.M.S. (1872)) began working in this field of WDR from 1816. Their results were used by the meteorologist and farmers (Philos (1816)).

Till 1936, the WDR gauges which are used in building hygrothermal behavior research were designed. As shown in Figure 1.2.1, generally there are two kinds of WDR gauges: free-standing gauges and wall mounted gauges. Free-standing gauges collect rain water from all 4 directions and are not fixed on the building façade. The WDR test results which obtained by using free-standing gauges are general value and are different from the results from wall mounted gauges which are restricted to the building with particular shape and dimensions. The WDR values obtained by different free-standing gauges have no obvious difference (Birkeland (1965)).

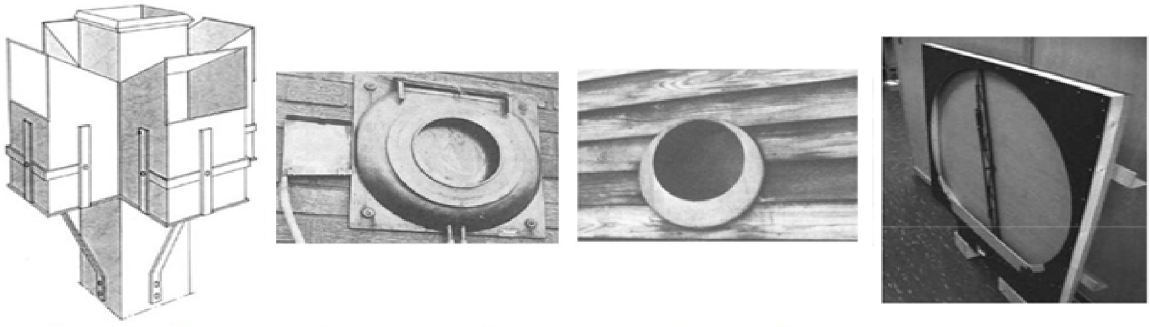

(a) Free-standing gauge (b) Wall-mounted gauge1 (c) Wall-mounted gauge2 (d) Wall-mounted gauge3

Figure 1.2.1: WDR gauges (Blocken & Carmeliet (2004))

There is no uniform production standard or process for wall mounted gauges. Therefore, the collection devices have different sizes and shapes. Researchers believe the essential factor that causes the collection error is the adhesion water on gauges' surface. During the short time drizzle, this error is more obvious. For a specific designed WDR gauge, the maximum amount of adhesion water is constant. The bigger WDR value is, the lower percentage the adhesion water accounts for. The runoff property of five materials including glass sheet, polymethyl-methacrylate (PMMA, acrylic), aluminium, stainless steel, and polished stainless steel were tested by Mr.Silvio Plescia and P.Eng (Plescia & Simpson (2009)). Although the glass has the best runoff performance, it is seldom chosen as the material for rain gauges. Because the gauge made by glass is too heavy and hard to install on building façades. Methods such as installing rotating wiper and spraying hydrophobic coating on the collection surface of rain gauges were applied to reduce the error caused by adhesion water (Hoegberg & van Mook F.J.R. 1999).

The full-scale WDR measurements have been carried out for different purposes in various locations. A low-rise VLIET test for the building in Figure 1.2.2a has been conducted by Blocken and Carmeliet (Blocken & Carmeliet (2005), Blocken & Carmeliet (2007*a*)) in Leuven to validate their WDR simulation result. Within the framework of wood frame wall performance research, Nore et al (Nore & Carmeliet (2007)) conducted a WDR measurement on the facades of a rectangular low-rise test building in Trondheim. As a part of a conservation study of historical monuments, the investigation of WDR impact on the east and west façades of one of the towers of Brodick Castle in Scotland was conducted by Kumaraperumal (Kumaraperumal & Mclean (2006)).

(a) VLIET test building in Leuven(Blocken & Carmeliet 2005)

(b) Test building in Trondheim(Nore (2006),Nore & Carmeliet (2007),)

(c) Brodick Castle in Scotland(Kumaraperumal & Mclean (2006))

Figure 1.2.2: Full scale measurements

As shown in Figure 1.2.2, these experiments have one thing in common: the frontage of the measured building or the frontage of the measured facade is an open ground which is helpful to eliminate the shelter effect by obstacles placed in the surrounding area.

Mr.Silvio Plescia and P.Eng monitored (Plescia & Simpson (2009)) have investigaed wind-driven rain (WDR) on 8 buildings in coastal British Columbia for two years. WDR data was collected to validate CFD models and verify the existing WDR models. As Figure 1.2.3 shows, the construction types of these 8 monitored buildings include low-rise buildings with and without overhang, high-rise buildings and long-slab buildings. As the geometric shapes of the residential buildings covered in this test research are more than the shapes included in the existing WDR calculation models and the CFD calculation results by Bert Blocken, the test database in this field was greatly enriched, and calculation coefficients used in WDR models was extended. The 8 buildings were selected from 35 buildings after the buildings' surroundings were investigated. 6 moderately sheltered buildings, 1 sheltered building and 1 exposed building were chosen. The wind-driven values achieved from the field measurements and values calculated by using empirical methods are listed in Table 1.6. Comparisons between test data and calculated data were made. The detailed analysis will be given in section 1.2.5.

Figure 1.2.3: Monitored buildings(Hua Ge 2008)

1.2.2 Semi-empirical study

The measurement results from the directional rain gauges (Figure 1.2.1a) indicate that the intensity of directional WDR increases approximately proportionally with wind speed and horizontal rainfall intensity. And this general rule leads to the development of semi-empirical method of directional WDR intensity investigation. Typically, two methods, namely the WDR index and the WDR relation, are employed for the approximate estimation of WDR intensity.

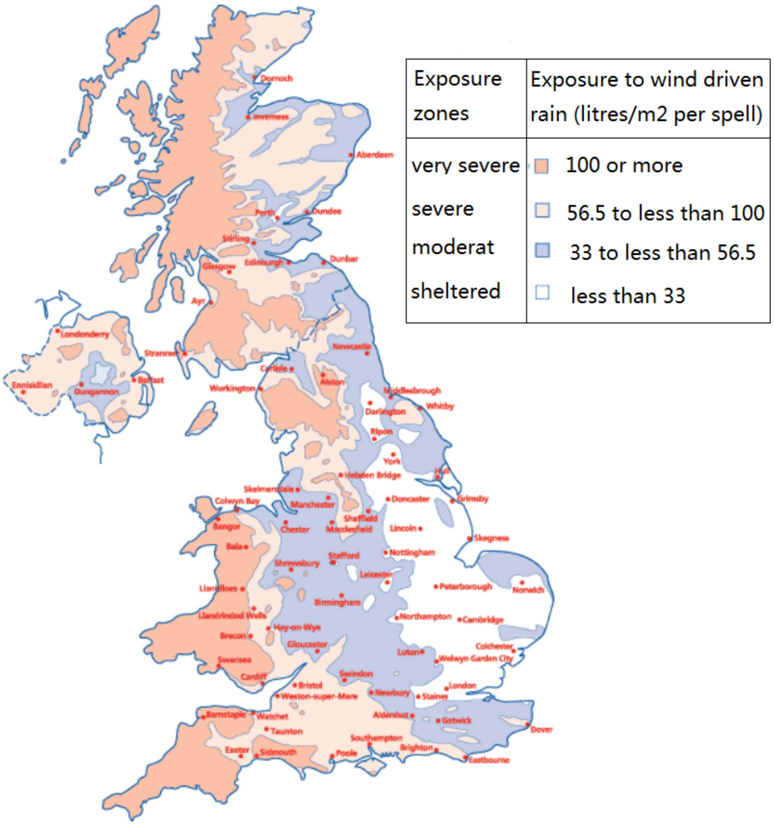

Figure 1.2.4: Wind-driven rain maps of the United Kingdom(Lacy (1971))

Wind-driven rain index

Wind-driven rain index is the WDR assessment within geographical scale. It can be used to give indications regarding the wetness of a certain location. In 1955, the first WDR map was completed for Norway (Hoppestad (1955)). Figure 1.2.4 indicates the mapping of wind-driven rain index in the UK. Similar to the one of UK's WDR maps which are also in Blocken's list were constructed for other countries (Lacy & Shellard 1962, Sauer 1987, Underwood & Meentemeyer 1998, Boyd 1963; Walsh 2010). Recently, WDR map study was carried out by Underwood for the contiguous United States. The study was based on data from 1961 to 1995 and from 182 stations across the United States (Underwood (1999)).

The WDR relation

The driving rain index (DRI) and the WDR map can provide the information of wetness at the place where the building locates. Research by Plescia & Simpson (2009) indicates that DRI is only an indicator of the potential wind-driven rain exposure of a specific wall, and the actual amount of driving rain impinged on the surface is largely influenced by the specific building environment and dimensions of the researched building.

The WDR relation is built on the observation that the WDR is related to the meteorological data got from weather stations which involves wind velocity, wind direction and horizontal rain intensity.

$$R_{wdr} = 0.222UR_h \tag{1.2.1}$$

Eq.1.2.1 gives the WDR calculation formula. In this equation, the wind direction is perpendicular to the windward facade. R_{wdr} is the WDR on building facade, (mm/h); R_h is the rain intensity on the horizontal ground; U is the average wind velocity, (m/s); 0.222 is the WDR average coefficient, (s/m). It applies to moderate rainfall intensity.

$$R_{wdr} = \alpha UR_h cos\theta \tag{1.2.2}$$

Eq.1.2.2 can be used to calculate the WDR on the wall in different direction. θ is the angle between the wind direction and the line normal to the wall. The WDR coefficient α is a comprehensive coefficient. The accurate WDR coefficient should present all the possible rainfall events and varying surroundings.

There are so far two simplified methods to estimate the WDR value on the building facade: ISO-WDR model and ASHW-WDR model. ISO-WDR model is given by EN ISO 15927-3(ISO (2009)).

ISO-WDR model The calculation formula and influencing parameters are shown in Table 1.2. $R_{airfield}$ is the quantity of WDR that would occur during one hour at a height of 10 meter above ground in the middle of an airfield. The WDR coefficient α is determined by four influencing factors according to different scales: the roughness factor R which takes into account the variability of the mean wind speed at the site due to upstream roughness of the terrain; the topography factor T ; the obstruction factor O which takes the shelter effect by the nearest obstacle into consideration and the wall factor W.

Table 1.2: WDR coefficient α

ISO-WDR model	ASHW-WDR model
$R_{wdr} = R_{airfield} \cdot R \cdot T \cdot O \cdot W$	$R_{wdr} = EHF \cdot TOF \cdot RDF \cdot DRF \cdot V(z) \cdot cos(\theta) \cdot R_h$
the roughness factor R	exposure and height factor EHF
the topography factor T	topography correction factor TOF
the obstruction factor O	the ratio of rain on a vertical plane to rain on a horizontal plane DRF
the wall factor W	the ratio of rain in the free wind to rain deposition on a building RDF

Table 1.3 shows the obstruction factors used in ISO-WDR model in which the obstruction factor is the function of the lengthwise distance. The obstruction buildings are considered as having the same geometry with the researched buildings and are right ahead of the researched buildings.

Table 1.3: Obstruction factors(ISO (2009))

Distance of obstruction from wall(m)	Obstruction factor O
4∼8	0.2
8∼ 15	0.3
15∼25	0.4
25∼40	0.5
40∼60	0.6
60∼80	0.7
80∼100	0.8
100∼120	0.9
>120	1.0

In Table 1.3, the buildings' packing density is only calculated from the lengthwise distance. The difference of WDR values caused by the broadwise distance between the obstructions is ignored. For the wind field simulation, the packing density as an important influencing parameter comprise of information of distance in both directions. This simplified method may cause significant errors in some cases. In addition, the shelter style is not taken into consideration in this obstruction. The location of the obstruction is simplified as right ahead of researched building with the same size and same geometry which do not exist in actual situations. In some cases, especially when the incoming wind flow is vertical to the researched facade, the shelter style plays an important role on the WDR.

In Figure 1.2.5 simplified wall factors for typical low-rise buildings in several geometries are presented. These wall factors were generated based on field measurement. The wall is vertically divided into several zones. There is wall coefficient for every zone. The all factors for positions that are easily exposed to more WDR such as corners and edges are not involved. In other words, the wall factors are not comprehensive enough, because it only can to a certain extent present vertical variability on building facade but not the horizontal variability.

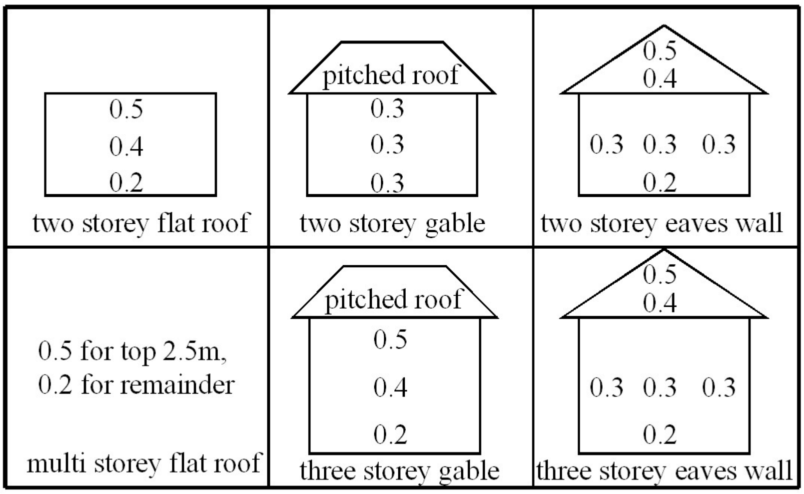

Figure 1.2.5: Wall factors (ISO 2009)

The verified coefficients (R, T, O, W) are constant for a given building and thusly the comprehensive WDR coefficient α does not change with time. The temporal characteristic of rainfall event and WDR cannot be represented.

ASHW-WDR model ASHRAE160p and WUFI 4.0 (Straube (2010)) have used ASHW-WDR model to estimate the rain intensity on a building facade. The model had been validated through field measurements.

The rain intensity calculation formula is given in Table 1.2. R_{vb} is the rain deposition rate on a vertical building facade (l/m^2h). EHF is exposure and height factor. EHF for the three different exposure classes and heights are summarized in Table 1.5.

Table 1.4: WDR coefficient α

ASHW-WDR model
$R_{wdr} = EHF \cdot TOF \cdot RDF \cdot DRF \cdot V(z) \cdot cos(\theta) \cdot R_h$
exposure and height factor EHF
topography correction factor TOF
the ratio of rain on a vertical plane to rain on a horizontal plane DRF
the ratio of rain in the free wind to rain deposition on a building RDF

Table 1.5: Wind velocity exposure and height factors (EHF) (Straube (2010))

Height(m)	Open country	Suburban	City center
1	0.72	0.56	0.44
3	0.84	0.74	0.65
5	0.91	0.84	0.78
7	0.95	0.91	0.88
10	1.00	1.00	1.00
20	1.10	1.19	1.28
30	1.17	1.32	1.49
50	1.25	1.50	1.78

TOF is a topography correction factor. It is the same with the factor T in ISO-WDR model.

RDF is the rain deposition factor. It is the ratio of rain in free wind to rain deposition on a building, which accounts for the effect of buildings' shape and size on rain deposition. The RDFs at various zones were obtained by measurements (Straube & Burnett (2005)). The values are shown in Figure 1.2.6.

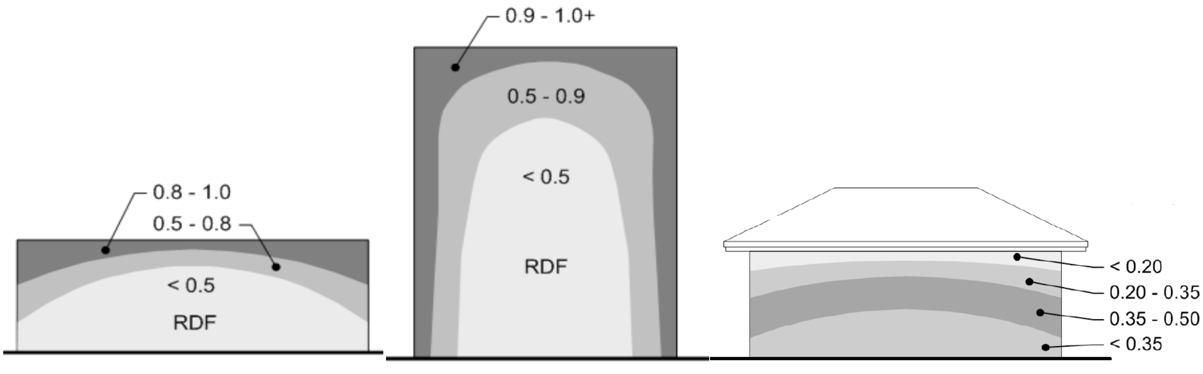

Figure 1.2.6: Rain deposition factor (RDF)(Straube (2010))

DRF is driving rain factor. It is the ratio of rain on a vertical plane to rain on a horizontal plane. For simple geometries, the DRF is equal to the inverse of the terminal drop velocity:

$$DRF = 1/V_{rainterminal} \tag{1.2.3}$$

where $V_{rainterminal}$ is the terminal raindrop velocity.

Field studies in Germany (kuenzel (1994)) and computer models (Choi (1994*a*), Choi (1994*b*)) have found that the values of DRF range from 0.20 to 0.25 for average conditions. However, DRF varies considerably according to different rainfall intensities and rain storm types. It can range from more than 0.5 for drizzle to as little as 0.15 for intense rainfall.

Compared to ISO-WDR model, the conclusions are drawn from following discussions:

As in the previous analysis, in ISO-WDR model the comprehensive WDR coefficient $\alpha = R \cdot T \cdot O \cdot W$ is a constant coefficient, which is independent from horizontal rain intensity R_h. In ASHW-WDR model, the comprehensive WDR coefficient $\alpha = EHF \cdot TOF \cdot RDF \cdot DRF$ is related to horizontal rain intensity R_h because of DRF, which is the function of raindrop terminal velocity. The temporal variability of WDR can be represented.

In ASHW-WDR model, the wall factors are more precise than in the method provided by ISO-WDR model. The facade is not simply divided by the height. The WDR distribution characteristic that rain water more easily falls and accumulates on the corner and edge of the building facade can be presented.

For the shelter effect, ASHW-WDR uses an average factor EHF. According to the average packing density of the location, the vertical wind velocities are revised. In real situation, the specific surrounding can cause significant influence on the wind field distribution.

1.2.3 Numerical study of WDR

It is convenient by using the numerical calculation to estimate WDR on the researched facade. It was not until quite recently that a method was established using Computational Fluid Dynamics (CFD) technique to calculate the amount of wind-driven rain on building facades. Sandberg (Sandberg (1974)) calculated the movements of raindrops around a building. Hilaire (Hilaire & Savina (1989)) computed the mean trajectories of drops in 2D wind fields around one or two buildings with a potential flow line method. Choi

(Choi (1994*a*)) began using the k-ε model to describe in detail the turbulent flows around various parallel buildings and computed the mean raindrop trajectories in these flows. Lakehal (Lakehal & Sini (1995)) used a heavy particle dispersion model to simulate hydrometeor trajectories in two-dimensional street canyon. Etyemezian (Etyemezian & Striegel (2000)) built a three-dimensional WDR model to calculate the rain intensity on a tall building facade.

The WDR simulation method developed by Bert Blocken and Jan Carmeliet provides researchers a method to obtain WDR on the facade of specific building with complicate geometry which has been validated by measurement. By using of a CFD package for wind field calculation and author-written Fortran 90 codes for the raindrop trajectories and the rain catch ratio calculation, the rain drops' movements were studied by Bert Blocken and Jan carmilie (Blocken & Carmeliet (2005)). In Bert Blocken's study, a certain rainfall event is decomposed into movement processes by several raindrop groups. Four typical geometry-shaped isolated buildings were simulated by using of this method (Blocken & Carmeliet (2006)). WDR distribution on these four facades were charted.

The WDR exposure of building site is significantly influenced by the local topography and surroundings. According to the evaluation of empirical method applicability by Mr.Silvio Plescia and P.Eng (Plescia & Simpson (2009)), the use of on-site weather data is very important to obtain more accurate WDR value. As the significant local variation of wind and rain conditions, the errors for specific wall could be as much as 90%. Shelter effect research is abundant on wind field, however there are only a few on rain trajectory, especially for three-dimensional investigation. Big spatial variety was ignored by two-dimensional research. Up to now, few documents about the shelter effect caused by surrounding buildings on WDR can be found.

1.2.4 Statistical study of WDR

Cornick, S.M and Lacasse (Cornick & Lacasse (2009)) introduced a statistical methodology to estimate the WDR loads and driving rain wind pressure. The historical climate data for specific locations (rainfall intensity, wind speed and wind direction) were used. This is a good methodology for determining the magnitude and likelihood of WDR loads and wind pressure loads which can be used in building envelope assembly test, and also be used in HAM tools as an extreme case with extreme climate conditions.

1.2.5 Discussions and conclusions

From the preceding description we can conclude:

- Although there is no industry norm for the production of the WDR gauges, the influencing factors that may result in errors have been analyzed and discussed. Research findings can give a good guidance for further researchers on design and production of WDR collection devices. Experimental WDR study results are affected by many factors: the selection of the test site, the design and the production of the rain collection gauges, and the installation of the rain gauges. The difficulties of the experimental-study result in the lack of wind-driven rain experimental data.
- The WDR map relies on the complete weather data, otherwise the application will lack credibility.
- The ISO-WDR model is a comprehensive WDR model, as it takes all the environment influencing factors into consideration. The roughness, the topography and the obstruction are all included in the correction coefficientα. As a rough estimation method, it can be easily used in the qualitative analysis. For HAM research on specific buildings, especially on the building with complex surroundings, the ISO-WDR model cannot estimate accurately WDR. In ISO-WDR model, the horizontal rain intensity is produced from statistic data based on wind and rain intensity data from weather station over years. Rain intensity value is averaged over periods with and without rainfall event instead of only during rain. As a result, WDR loads are always underestimated by ISO-WDR model.
- Compared to ISO-WDR model, ASHW-WDR model can estimate WDR values from a specific rainfall event. The driving rain factor DRF builds a relation between the WDR coefficient and the concrete rainfall event. The comprehensive factor α is not a constant, but a temporal coefficient which changes with different horizontal rain intensities. The rain deposition factor RDF is not only vertically divided but also better embodies the variability on edge and in corners. The shelter effect is neglected because of the lack of obstruction coefficient.
- The WDR simulation technique developed by Bert Blocken and Jan Carmeliet (Blocken & Carmeliet (2002)) can accurately estimate WDR value. The detailed information of the researched building which involve the complicated building geometry and the complicated building environment can be reproduced by CFD model. The results can represent the spatial and temporal characteristics of WDR on the building facade. However this calculation procedure is complicated to accomplish. A good understanding of fluid dynamics knowledge and good mastering

of CFD simulation skill are necessary for the calculator, and moreover, it is a time-consuming as well as a labor-consuming process. The results of WDR simulation can only be used to estimate WDR values on specific building facades in specific environment and have limitations for wider application in HAM tools.

Table 1.6: Comparison of the catch ratio values

	Position	1	2	3	4
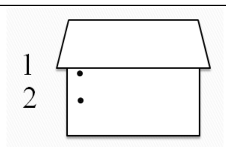	Field measurement	0.033	0.159	-	-
	ISO-WDR	0.3	0.3	-	-
	ASHW-WDR	0.2	0.2	-	-
	Blocken	-	-	-	-
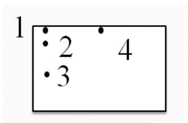	Field measurement	0.008	0.067	0.078	0.002
	ISO-WDR	0.5	0.5	0.4	0.5
	ASHW-WDR	-	-	-	-
	Blocken	-	-	-	-
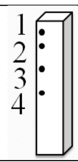	Field measurement	0.504	0.326	0.143	0.084
	ISO-WDR	0.5	0.2	0.2	0.2
	ASHW-WDR	0.9~1.0	0.9~1.0	0.9~1.0	0.9~1.0
	Blocken	0.736	-	-	0
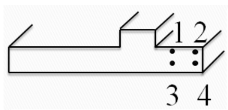	Field measurement	0.209	0.360	0.122	0.314
	ISO-WDR	-	-	-	-
	ASHW-WDR	0.8~1.0	<0.5	0.8~1.0	0.8~1.0
	Blocken	0.501	0.058	0.666	0.101

(Field measurement data is from Plescia & Simpson (2009) ; ISO-WDR data is from ISO (2009); ASHW-WDR data is from Straube (2010); Blocken data is from Blocken & Carmeliet (2006))

- Catch ratio values from different sources (shown in table 1.6) have a considerable difference. The field measurement data were collected by Mr. Silvio Plescia and P.Eng in Metro Vancouver from November 2006 to July 2008. The ISO-WDR model and ASHW-WDR model are generalized from long-term measurement data. Blocken was obtained by CFD calculation. From the data listed in Table 1.6, it can be found that in generally the catch ratios from field measurement are smaller than the data from other sources. Although Mr. Silvio Plescia and P.Eng had made efforts to choose buildings with higher exposure, only moderate sheltered buildings were selected. The reduction of rain fall exposure may be caused by the surrounding obstacles. On the same position, the catch ratios differ greatly. It is hard to find any rules from those differences. Although the buildings has similar geometries in Table 1.6, their dimensions are not the same. This maybe one of the reasons for the variety. The characteristics of a rainfall event including rainfall intensity, frequency, and wind velocity, wind direction have effects on the catch ratio value. As the catch ratio values from different models (ISO-WDR and ASHW-WDR) and measurements were analyzed based on data from different regions, the variety also may be caused by the geographical difference of test sites.

1.3 The significance of wind-driven rain research in urban areas

1.3.1 Urbanization und microclimate in urban areas

According to a research by United Nations (2010), over 64% of new population lived in cities from 1950 to 2010. As of 2010, more than 50% population in the world, about 3.5 billion, lives in urban towns and cities. It is foreseeable that, the growth of urbanization will continue in the next few decades. By 2045, every two out of three persons are expected to live in urbanized areas. Figure 1.3.1 shows the trend towards urbanization all over the world. The ongoing urbanization results in the growing interest in the study of urban climate and its impact on energy usage. The most important microclimate is the so-called urban heat island (UHI) which makes temperature in the urban areas higher than that in the suburbs.

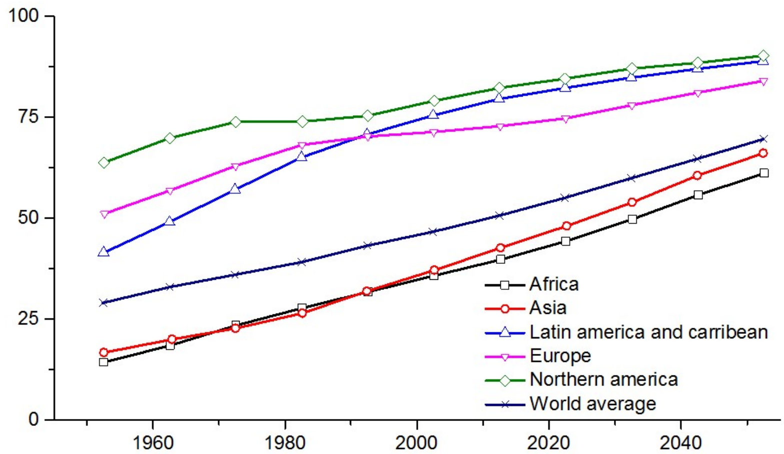

Figure 1.3.1: Trend towards urbanization all over the world

Figure 1.3.2 indicates that the UHI intensity in the areas with frequent human activities is much higher than in areas of less human activity.

Possible reasons for urban heat island have been summarized by :

- Trapped short and long-wave radiation in between buildings.

- Decreased long-wave radiative heat losses due to reduced sky-view factors.
- Increased storage of sensible heat in the construction materials.
- Anthropogenic heat released from combustion of fuels (domestic heating, traffic).
- Reduced potential for evapotranspiration, which implies that energy is converted into sensible rather than latent heat.
- Reduced convective heat removal due to the reduction of wind speed.

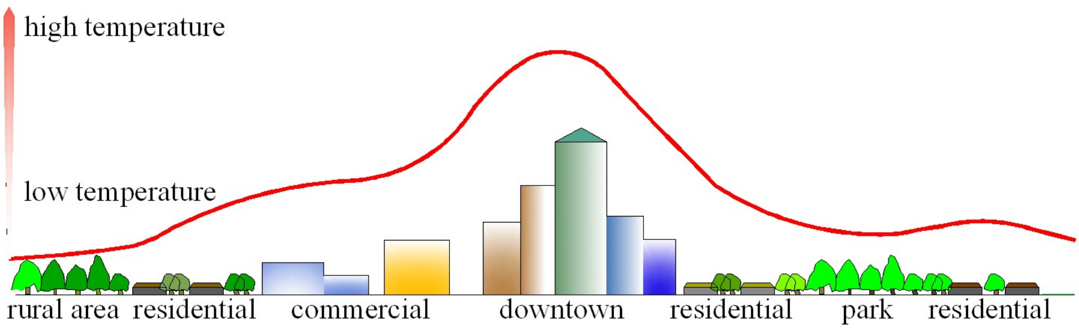

Figure 1.3.2: Temperature distribution of urban heat island

Urban heat island is regarded for the change of local and global climate and is important with regard to livability. In the process of urbanization, the emergence of large cities and metropolitan regions expands the impact of urban heat islands. A large number of emerging cities result in increasing demand of energy, which may lead human to enter a non-sustainable development process. In this section, due to its rapid development and its potential influence on the global climate change, as well as the application potential of WDR in building energy saving in China, a special attention is given to the ongoing urbanization process in China.

1.3.2 WDR research on the process of China's urbanization

The reasons of WDR research on the process of China's urbanization are:

1) The rapid development of urbanization in China provides an opportunity for the applications of urban physics research which includes the research of WDR.

2) In China, like in other countries of the world, there is a research gap in the research of WDR in urban areas.

The ongoing process and challenge of China's Urbanization

China's urbanization started from the late seventies, and rapid developed in the past 20 years. In present, China's urbanization rate is 51.3%, which is still in a rapid developing stage (shown as in Figure 3.2.3). In this stage, urbanization shows the agglomeration effect and small cities begin expanding. At the current pace of development, in the next few decades, there will be 242 cities with a population of over one million, and 9 cities with a population of more than 10 million in China.

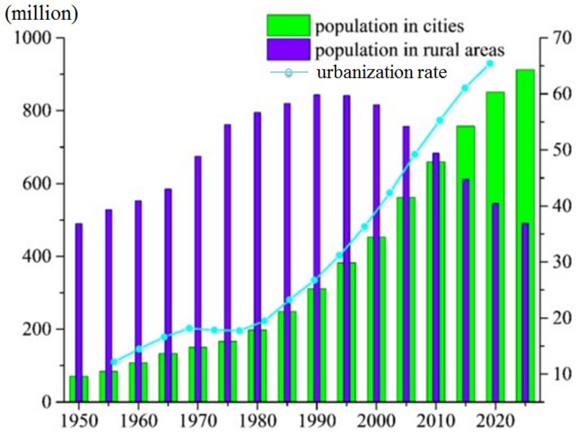

(a) China's urbanization rate and its population in city and rural areas

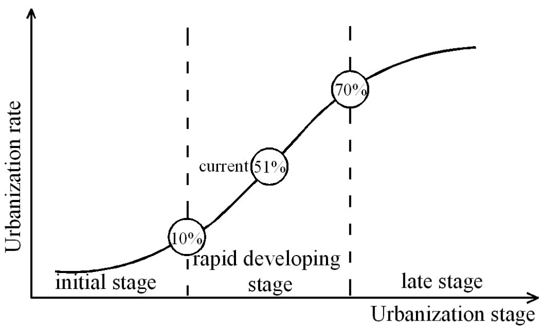

(b) Urbanization stage

Figure 1.3.3: Urbanization in China (source: http://www.people.com.cn/)

In China, urbanization has the following features:

- Some large cities have a high level of urbanization. In these cities, due to the substantial increase in population, part of the population gradually shift to suburbs. Counter-urbanization in this period triggers a rapid development of the suburbs.
- In some small cities, the urbanization level has rapidly raised and the city scale will continue to expand.

The expanding of UHI affected areas makes the boundary between cities and suburbs no longer obvious. Thus the cooling effect of green spaces in suburb will be weakened. This will cause a rapid growing demand of air-conditioning in summer. In the past ten years, the holding of air-conditioning increases from 261 million units (1995) to 900 million units (2010). Figure 3.2.4(a) shows the use of air-conditioning in China and Figure 3.2.4(b) indicates the energy consumption of air conditioning in China. As can be seen, in 2008 air-conditioning energy consumption is 6% in China's building energy consumption and it is believed to continue growing with the continuously increasing of air conditional demand. How to control the rapid growth in residential air conditioning energy consumption has become a problem for Chinese building energy conservation that needs to be solved.

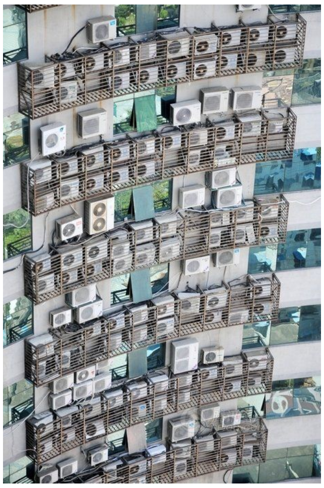

(a) Air conditioner usage

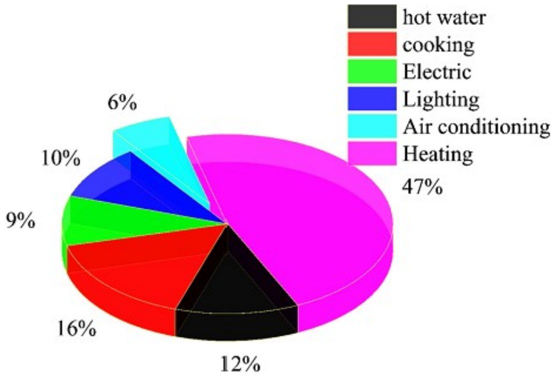

(b) Building energy consumption in China (Jiang Yi,2008)

Figure 1.3.4: The use and the energy consumption of air-conditioning in China

Energy saving potential of buildings in the China's urbanization

In engineering practice, passive cooling methods such as green and water storage roofs (shown as Figure 1.3.5) can be used to reduce the cooling energy demand in summer. For buildings rainfall can be seen as a natural passive cooling method. Rainfall can not only reduce the surface temperature of the building, but also can effectively change the thermo-hydro performance of facade by absorbing and storing moisture. The effect of WDR is supposed to reduce the usage of air conditioning in rainy places in summer. The energy-saving potential caused by WDR on buildings is rarely mentioned or integrated into existing energy analysis software.

The possible application of WDR in building energy saving can be achieved by:

- Being embedded in existing building energy simulation software to make it more comprehensive.
- Providing a theoretical basis for the study of new building components.

As mentioned in previous parts, the urbanization of China will promote the emergence of many city circles (shown in Figure 1.3.6a). These cities will face a challenge of high cooling energy demand in summer. It is worth highlighting that most of these new city cycles locate in areas of China with relatively abundant rainfall, shown as Figure 1.3.6a.

Thus, the passive cooling effect of WDR has practical significance to reduce building energy consumption in summer.

Figure 1.3.5: Passive cooling application (source:http://wall.alphacoders.com/)

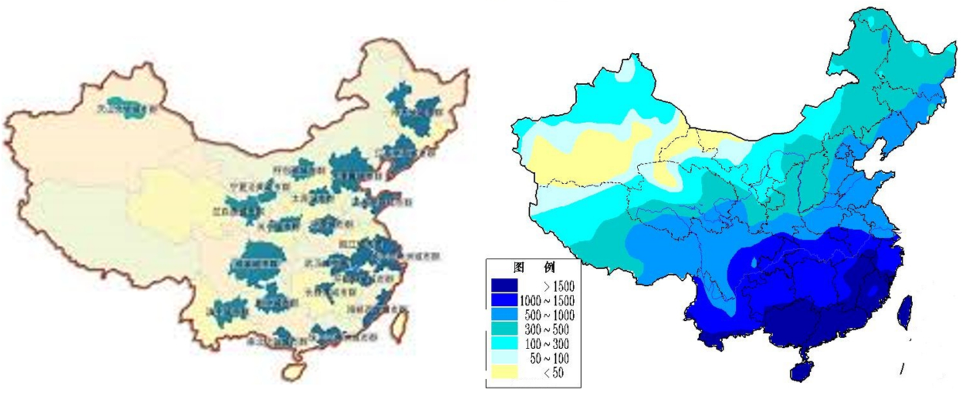

(a) City cycles in China (b) Annual rainfall distribution in China

Figure 1.3.6: City cycles and annual rainfall distribution in China (source:http://www.gov.cn/)

The application of WDR research in building energy simulation

Building energy simulation (BES) tools can be used to design and optimize building envelope. Figure 1.3.7 shows the implementation of wind engineering in BES. In addition to the transfer process mentioned in the literature on convective heat and natural ventilation, wind engineering applications in building energy simulation should also include wind-driven rain. The implementation of WDR in BES is a multi-physics process which includes the mass and heat transfer process. In most of the energy analysis software, the impact of WDR in BES is simplified or neglected. The results cannot be trusted or may cause the discrepancy with the actual situation, especially in the rainy regions in summer.

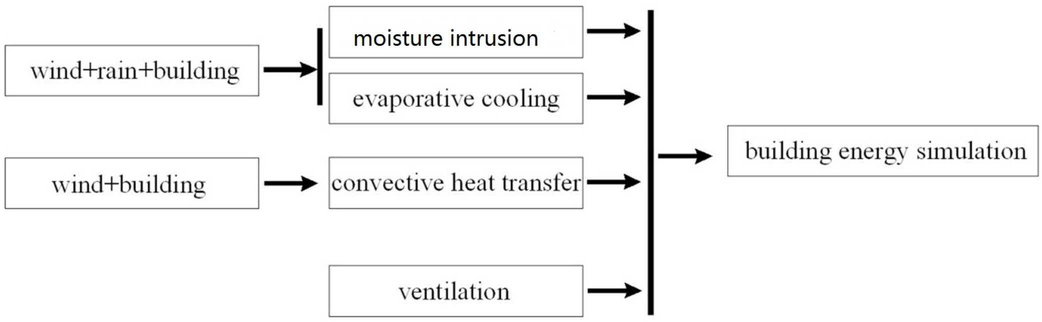

Figure 1.3.7: Implementation of wind engineering in BES

From this perspective, it is necessary to add the ongoing works of WDR and moisture transfer in building components when conducting the building energy simulation in order to obtain a compressive knowledge of building energy consumption. In this study, how to embed wind-driven rain research into building energy simulation analysis will be our target.

1.4 Introduction to the new WDR model research

1.4.1 Objective of this work

Due to the lack of research on WDR in the urban areas, the subject of this study is the shelter effect on WDR in the urban environment.

- The first objective is to study the shelter effect on WDR on buildings in urban blocks. Two typical urban street arrangements and three densities are taken as research objects. The analysis includes the atmospheric boundary layer influence on WDR, the wind field and rain drops' movement in a street canyon, and the shelter effect on WDR catch ratio distribution.

- The second objective is to propose a WDR calculation methodology which can estimate the WDR amount without complicate CFD simulation procedures.

1.4.2 Research methodologies

Measurement

Two buildings still under construction are chosen for experimental study. Rain water impinging on building facades is collected by rain gauges which have been distributed over both unobstructed and obstructed building facades to obtain enough data to investigate spatial variety and shelter rate. The local wind velocity and local horizontal rain intensity have been obtained by a moving climate station.

Validation of wind field and rain trajectory calculation

The CFD package Fluent is used to simulate the wind field around an urban street. The turbulent model which is used to build an atmospheric wind field was validated by test data obtained from a wind-tunnel test carried out by Stathopoulos and Wu (Stathopoulos & Wu (1995)).

The rain drop scenario simulation is carried out with Fluent software. The raindrops as the discrete phase cooperates with the calculated wind field. A cluster of rain drops with different diameters fall from the clouds zone with different terminal velocities. The raindrops' movement has been calculated based on the wind field obtained by CFD simulation.

Statistical analysis

Statistical methods have been used to analyze the correlations between WDR and influencing factors. The main influencing factors are selected by correlation analysis. The regression analysis of the main influencing factors and of WDR catch ratio has been performed. The WDR calculation coefficient table has been formulated.

1.5 Outline of the thesis

In chapter 2, the simulation of flow in atmospheric boundary layer (ABL) has been conducted. Meanwhile, ABL's effect on the catch ratio in the horizontal direction has been assessed.

In chapter 3, the validations of the WDR models are performed. Data from validated CFD model are used to compare with data from measurement which was designed and organized by the author. The shelter effect for the test buildings is analyzed.

In chapter 4, the shelter effect for WDR on the building facade is systematically investigated by applying a parameterized urban arrangement and urban density. The detailed wind field characteristics in the street canyon and the rain drop movement in the street canyon are investigated. The rules of the catch ratio on building facade and the catch ratios' variety are studied.

In chapter 5, the correlation between catch ratio and influencing factors is studied. The main influencing factors are selected for regression analysis.

In chapter 6, a program is designed to implement this new WDR model. Multidimensional WDR database calculated by the author is introduced. A case study is used to illustrate the application steps of the new WDR model.

In chapter 7, perspectives of WDR study is given.